CHARACTERIZATION OF THRUST FAULTS ON THE MOON USING THERMOELASTIC STRESS CALCULATIONS AND 3D VISUALIZATIONS J. D. Clark[1] and J. M. Hurtado Jr[2], [1,2]University of Texas at El Paso, Department of Geological Sciences and UTEP Center for Space Exploration Technology Research, 500 West University Avenue, El Paso, Texas 79968-05555, [1]jdclark@miners.utep.edu, [2]jhurtado@utep.edu.

Introduction: It is well established that the Moon's mantle and crust are cooling from an initially molten state [1]. Due to this cooling, the Moon's crust has contracted, creating thrust faults that manifest themselves as surface ruptures and lobate scarps [1,2]. According to Binder and Lange [3], the lunar radius has decreased by ~5 km due to this process. More recently, estimates of the strain released by the formation of lunar thrust fault scarps have suggested a much smaller decrease in lunar radius of ~100 m [2]. Due to the large variability between these studies, further investigation is needed to better constrain the amount of crustal shortening.

Early studies [4] of lobate scarps were conducted using images from the Apollo Panoramic Camera, leaving research confined to the equatorial region. With new, high-resolution images from the Lunar Reconnaissance Orbiter camera (LROC), the global spatial distribution of lobate scarps can be mapped [2], and the topography of the lunar surface can be viewed in greater detail than possible before, allowing quantitative structural measurements to be made of the scarps and the faults that produced them. These structural measurements can be used in thermoelastic stress calculations to determine better constraints on the amount of crustal shortening. Furthermore, crater counts on surfaces cut by the fault can yield age constraints for the scarps, revealing the timing of contractional faulting on the Moon. The objective of this study is to demonstrate a methodology for placing better constraints on the amount and timing of shortening of the lunar crust to improve our understanding of the stress state of the Moon.

Scarp Morphology: Based on their generally crisp appearance and the lack of superimposed, large-diameter impact craters, many of the lobate scarps are among the youngest (≤~500 Myr) landforms on the Moon [2,5]. These scarps are interpreted to be the manifestation of reverse slip on faults [1]. Characteristically, lobate scarps consist of steep scarp faces, and they cross cut small impact craters [2]. The lunar thrust fault scarps have a linear or curvilinear asymmetric shape with arcuate fault surfaces [2,5]. Typically, the scarps consist of a series of smaller, connected subscarps called complexes [1]. Previously investigated scarp complexes span lengths of up to ~10 km, occurring in a series of up to 10 subscarps, and generally having maximum relief of <~100 m [2,4]. Previously undetected scarps are now being found [2], with the help of LROC images, at higher latitudes than before (≥60˚). The distribution of scarps at high, middle, and low latitudes on both sides of the Moon suggests that thrust faults are globally distributed [2].

Fault Mechanics: Mohr-Coulomb failure laws [6] and Andersonian fault dynamics theory [7] can assist in understanding the compressional stress state of the Moon. Thermoelastic stress calculations can yield estimates for the amount of stress needed to rupture thrust faults like the ones observed in remotely-sensed imagery. These computations can also be used to quantify the amount of crustal shortening.

The compressional, tangential stress (σ) needed to produce a thrust fault can be calculated using [4]:

$$\sigma \geq K\rho g z + S \quad (1),$$

where ρ is the density of the material (mare basalts, ρ = 3.2 g/cm^2; anorthositic highlands, ρ = 2.5 g/cm^2 [8]), g is the gravitational acceleration (163.3 cm/s^2 for the Moon [1]), z is the depth of faulting, and S is the crushing strength of the rock (4±3 kbar [9]). The parameter K is a function of the coefficient of friction (F) and is given by given by [4]:

$$K = \frac{\sqrt{1+F^2}+F}{\sqrt{1+F^2}-F} \quad (2).$$

Eqs. (1) and (2) provide constraints on the amount of compressional stress to create the fault scarps. Results from Eq. (1) can be plotted on a map and draped over topographic data and LROC images of the scarps to reveal the distribution of compressional stresses and show if the stress varies or is spatially uniform.

Geometric quantities, such as the maximum depth of faulting (Z) and the fault dip angle (θ) can be computed using [4]:

$$Z = R \tan 0.63\psi \quad (3)$$

$$\theta = \frac{2}{\pi}\psi \quad (4),$$

where R is the radius of the scarp and ψ is the half-angle of the curved scarp. These parameters can be used to create geologic cross-sections and 3D visualizations for use in estimating the amount of shortening accommodated by the faults. Previous research [2,4] based on morphology and cross-cutting relationships has shown that lunar thrust faults have a low dip angle, averaging 21˚±0.5˚. The maximum depth of faulting is important since it is an open question if faults are confined to the lunar regolith or if they penetrate to greater depths. Previous research has found that the thrust faults are confined to the regolith, having an average depth of ~6 km [4].

Study Area: This project presents structural analyses of two sites which were chosen because they are geologically diverse, unexplored areas that contain lobate scarps: (1) Apollo and Korolev craters near South Pole Aitken Basin; and (2) the area between Mare Imbrium and Mare Serenitatis, near the Apollo 15 landing site. Study area 1 is located on the farside of the Moon just north of the South Pole Aitken (SPA) Basin. This area primarily consists of cratered anorthositic highlands with some basaltic material around Apollo crater. Study area 2 comprises cratered anorthositic highlands and mare basalt. It contains more basaltic rock than study area 1 due to its proximity to Mare Imbrium and Mare Serenitatis.

Methodology: Lobate scarps were identified using LROC Narrow Angle Camera (NAC) and Wide Angle Camera (WAC) images. Geologic maps were created by photointerpretive methods using *ENVI* and *ArcMap* software. Using *ArcMap*, we also take measurements of the scarp R and ψ values. These parameters were then used in Eqs. (1)-(4), which were implemented with a *MATLAB* code.

For each scarp locality, a 3D visualization and geologic cross-section was created using *Fledermaus* and *3D Move* software, respectively. Using *Fledermaus*, NAC images were draped over the Lunar Orbiter Laser Altimeter (LOLA) digital elevation model (DEM) (Fig. 1 shows an example). The resulting 3D visualizations allow us to view the scarps and the surrounding terrain in perspective for mapping purposes. Furthermore, we can make structural measurements (i.e. strike and dip) using the three-point method from the terrain visualizations. Photogeologic maps created in *ArcMap* are imported to *3-D Move* to construct geologic cross-sections. These cross-sections show the geometry of the fault scarps and assist in placing constraints on the amount of shortening.

Finally, we conduct crater counting with the aid of the *CraterTools* extension to *ArcMap* [10] in order to constrain the ages of the fault scarps. *CraterTools* allows users to digitize crater diameters and perform statistical analyses of the crater size-frequency distribution over a selected area to generate absolute ages of surfaces [10]. Knowing the absolute age of surfaces cut by the scarps will assist in determining approximate timing of faulting.

Results: To date, 10 previously undetected scarps have been found collectively in both study areas. The scarps located between Apollo and Korolev craters (study area 1) have an average dip of 15.9˚ and a depth of 0.26 km (Table 1). Those adjacent to the Apollo 15 landing site (study area 2), have an average dip of 18.8˚ and a depth of 0.33 km (Table 1).

Summary: Preliminary results from the far and near side of the Moon show that arcuate scarps are the result of shallow, low-angle thrust faults. This ongoing study of identified and previously undetected faults scarps will better constrain the amount of crustal shortening and improve our understanding of the stress state of the Moon.

References: [1] Binder, A.B. (1982) *Moon and Planets*, 26, 117-133. [2] Watters, T. R. et al. (2010) *Science*, 329, 936-940. [3] Binder, A.B. and Lange, M.A. (1980) *Journal of Geophysical Research*, 85, 3194-3208. [4] Binder, A.B. and Gunga, H. C. (1985) *Icarus*, 63, 421-441. [5] Binder, A.B. (1986) *Papers Presented to the Conference on the Origin of the Moon*, 425-433. [6] Clark, S.P., Jr. (1966) *Handbook of Physical Constants* (Geological Society of America Memoir, 97, 586. [7] Anderson, E.M. (1951) Oliver & Boyd (Edinburgh), 206. [8] Lee, D. C. et al. (1997) *Science*, 278, 5340, 1098-1103. [9] Binder, A.B. (1986) *Papers Presented to the Conference on the Origin of the Moon*, 425-433. [10] Kneissl, T. et al. (2010) LPS MMXI, Abstract #1638.

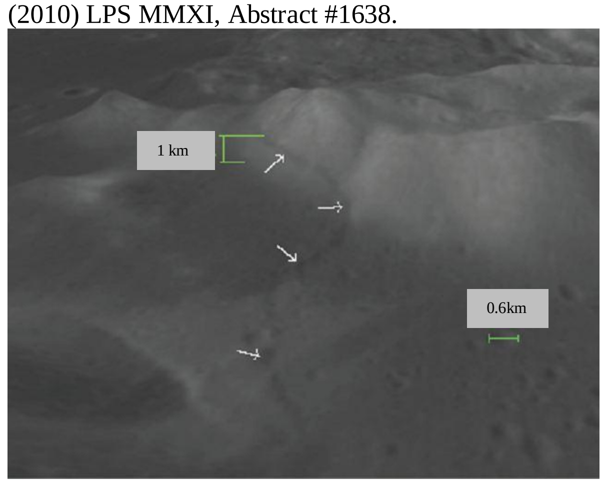

Figure 1. *Oblique view of WAC image (M119645947ME; 100-m/pixel resolution) draped over the LOLA DEM (1-m/pixel resolution) showing the Lee-Lincoln scarp (white arrows). 3D visualization produced with Fledermaus software. Illumination from the southwest. View to the north.*

Fault No.	R (km)	Ψ (deg)	θ (deg)	Z (km)
1-1	0.63	26.1	16.6	0.27
1-2	1.19	22.2	14.1	0.30
1-3	1.08	27.2	17.3	0.33
1-4	0.44	24.3	15.4	0.12
2-2	1.20	28.9	18.4	0.39
2-3	0.78	29.4	18.7	0.26
2-4	0.97	30.1	19.2	0.33

Table 1. *Preliminary thermoelastic calculation results. Faults are categorized by study area first, then fault number (i.e. 1-2, is from study area 1 and is fault 2).*